

# Synthesis, electrochemistry and First Principles Calculation studies of layered Li-Ni-Ti-O compounds

Kisuk Kang<sup>+</sup>, Dany Carlier, John Reed, Elena M. Arroyo, Meng Shirley Ying<sup>\*</sup> and Gerbrand Ceder<sup>++</sup>

Department of Materials Science & Engineering, Massachusetts Institute of Technology, 77 Mass. Ave, Cambridge, MA 02139, USA

<sup>\*</sup> Singapore-MIT Alliance, National University of Singapore, Science Drive 4, Singapore 117543

**Abstract** — New layered cathode materials,  $\text{Li}_{0.9}\text{Ni}_{0.45}\text{Ti}_{0.55}\text{O}_2$ , were synthesized by means of ion-exchange from  $\text{Na}_{0.9}\text{Ni}_{0.45}\text{Ti}_{0.55}\text{O}_2$ . The degree of cation disordering in the material depends critically on the synthesis conditions. Longer times and higher temperatures in the ion-exchange process induced more cation disordering. However, the partially disordered phase showed better capacity retention than the least disordered phase. First principles calculations indicated this could be attributed to the migration of  $\text{Ti}^{+4}$  into the Li layer during the electrochemical testing, which seems to depend sensitively on the  $\text{Ni}^{+2}$ - $\text{Ti}^{+4}$  configuration in the transition metal layer. The poor conductivity of this material could also be the reason for its low specific capacity according to the Density of States (DOS) obtained from first principles calculations indicating that only Ni participates in the electronic conductivity.

**Index Terms**—Ion Exchange, Li cathode, First Principles Calculation.

## I. INTRODUCTION

We investigate the structure and electrochemical behavior of  $\text{Li}_{0.9}\text{Ni}_{0.45}\text{Ti}_{0.55}\text{O}_2$  using a combination of experiments and first principles calculations. It was recently demonstrated experimentally [1,2] and theoretically [3] that in  $\text{LiNi}_{0.5}\text{Mn}_{0.5}\text{O}_2$ , Ni can be cycled from +2 to +4 in a reasonable voltage range while  $\text{Mn}^{4+}$  remains inactive. The restriction of Mn to the +4 state is what gives this material its high stability, as more reduced valence states of Mn are

prone to migration [4]. As a potential analogue to  $\text{Li}(\text{Ni}^{+2}\text{Mn}^{4+})\text{O}_2$ , we have investigated  $\text{Li}(\text{Ni}^{+2}\text{Ti}^{4+})\text{O}_2$ . This material is expected to be more difficult to synthesize in the layered R3-m structure as both  $\text{Ni}^{+2}$  and  $\text{Ti}^{4+}$  have a relatively large ionic size, making them prone to mixing into the Li layer [5]. Indeed, a direct high temperature synthesis effort [6] of  $\text{Li}_x(\text{Ni}_{1-y}\text{Ti}_y)\text{O}_2$  led to disordered rocksalt structures for  $y \geq 0.4$ .

Several investigators have doped small amounts of Ti into  $\text{LiNiO}_2$  [6-8] in some cases leading to an improved capacity over undoped  $\text{LiNiO}_2$ . In this work, we attempt to synthesize layered  $\text{Li}(\text{Ni,Ti})\text{O}_2$  by ion-exchange from the  $\text{Na}(\text{Ni,Ti})\text{O}_2$  precursor. Even though we have been successful in this, the experimental results and first principles calculations all point towards a material that is rather prone to transition metal cation migration into the Li layer.

## II. EXPERIMENTAL

The Na-phase ( $\text{Na}_{0.9}\text{Ni}_{0.45}\text{Ti}_{0.55}\text{O}_2$ ) used as starting material for the ion exchange was prepared by solid-state reaction from  $\text{Na}_2\text{CO}_3$  (98+%, Aldrich),  $\text{NiO}$  (99.3%, J.T. Baker) and  $\text{TiO}_2$  anatase (99.9+%, Aldrich). The appropriate amounts of these starting materials were wet ball-milled for 1 day. After drying, this mixture was calcined at 750°C for several hours, ground using a mortar, and pressed into a pellet shape. The pellet was heated at 1000°C for 14 hours in air or Ar (but both the results were same). An excess amount of  $\text{Na}_2\text{CO}_3$  (10 mol%) was added to compensate for the loss because of the volatilization of sodium at high temperature.

The obtained Na-containing green powder was wet ball-milled before ion exchange to reduce the particle size. The powder was added to a solution of 5M LiBr 10 times excess in 120°C hexanol for 48 hours, or boiling hexanol for 12, 20 or 48 hours. After ion exchange, the mixture was filtered to recover the powder and rinsed with hexanol,

Manuscript received October 30, 2003. This work was supported by Assistant Secretary for Energy Efficiency and Renewable Energy, Office of FreedomCAR and Vehicle Technologies of the U.S. Department of Energy under Contract No. DE-AC03-76SF00098, Subcontract No. 6517748 with the Lawrence Berkeley National Laboratory and by the US-France cooperative agreement NSF-INT-0003799

<sup>+</sup>Kisuk Kang is a Ph. D student in Department of Materials Science and Engineering at MIT. (e-mail: matlgen1@mit.edu).

<sup>++</sup>Gerbrand Ceder is a faculty in Department of Materials Science and Engineering at MIT. (corresponding author phone: 1-617-253-1581, fax: 617-258-6534, e-mail: gceder@mit.edu)

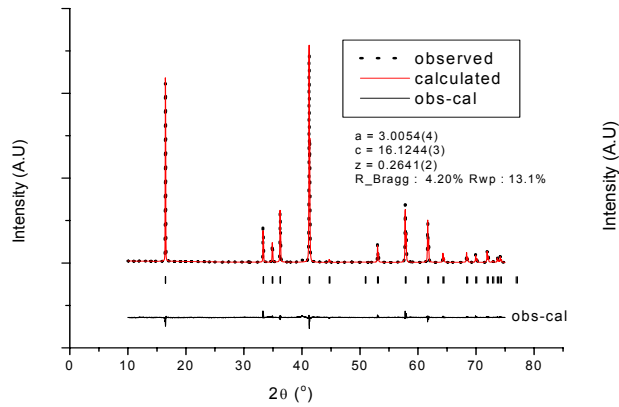


**Fig. 1** XRD pattern and Rietveld refinement of  $\text{Na}_{0.9}\text{Ni}_{0.45}\text{Ti}_{0.55}\text{O}_2$  (a and c are the lattice parameters and z is the atomic position of oxygen along the c axis.)

distilled water and ethanol several times. Finally, the obtained Li-containing light green powder was dried in the air for a day in oven.

The lithium cells were configured in the following way: Li/1M  $\text{LiPF}_6$  in EC: DMC=1:1 (Merck) /  $\text{Li}_{0.9}\text{Ni}_{0.45}\text{Ti}_{0.55}\text{O}_2$  with carbon black (15 wt%) used as conductive agent and polyethylenetetrafluoride (PTFE)(5 wt%) as binder. Cells were assembled in an argon-filled glove box and cycled at room temperature using a Maccor 2200 operating in galvanostatic mode. The electrochemical performances of the samples were evaluated upon cycling in the 2.5-4.8V potential window at C/10, C/30 and C/50 rate.

The XRD pattern was recorded using a Rigaku diffractometer equipped with a  $\text{Cu-K}\alpha$  radiation by step scanning ( $0.02$  or  $0.01^\circ/10\text{sec}$ ) in the  $2\theta$  range of  $10$ - $75^\circ$ . The structure was refined with Full-Prof. XRD samples were prepared by spaying the powder to the holder in order to prevent a preferred orientation of the material

### III. RESULTS AND DISCUSSION

The XRD pattern and lattice parameters of  $\text{Na}_{0.9}\text{Ni}_{0.45}\text{Ti}_{0.55}\text{O}_2$  is shown in Figure 1. Below the measured diffraction pattern are the calculated pattern for the  $\alpha\text{-NaFeO}_2$  (R-3m) structure with transition metals (Ni, Ti) in 3b (0,0,0.5) sites, Na in 3a (0,0,0) sites and O in 6c (0,0,z) sites, and the difference between the calculated and observed patterns. Rietveld refinement indicates less than 4% of cation mixing. No additional peaks suggesting ordering between transition metals (Ni and Ti) or between Na and vacancies have been observed. The refined structure parameters are in good agreement with previous studies [10,11]. Figure 2 shows the XRD pattern of the compound  $\text{Li}_{0.9}\text{Ni}_{0.45}\text{Ti}_{0.55}\text{O}_2$ . It is similar to that of  $\text{LiCoO}_2$  ( $\alpha\text{-NaFeO}_2$  type, space group R3-m) and can be indexed as a hexagonal

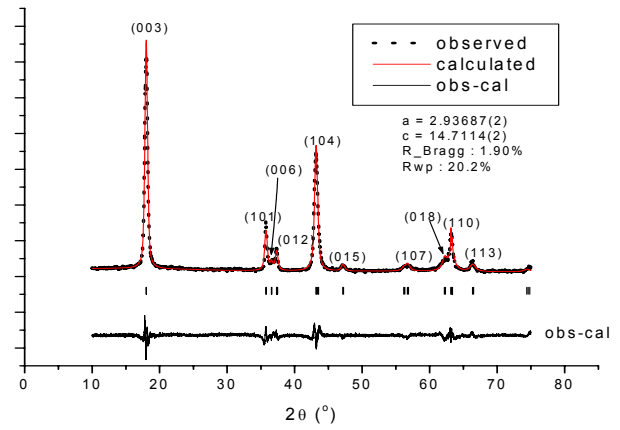


**Fig. 2** Full pattern matching of  $\text{Li}_{0.9}\text{Ni}_{0.45}\text{Ti}_{0.55}\text{O}_2$

lattice. No superlattice peaks from Li-vacancy ordering and Ni-Ti ordering are present in XRD pattern. The structural parameters, obtained from full pattern matching, are in reasonable agreement with the trends obtained by Kim and Amine [12] for lower Ti contents [9]. The composition was determined with ICP to be  $\text{Li}_{0.79}\text{Na}_{0.12}\text{Ni}_{0.46}\text{Ti}_{0.54}\text{O}_{1.995}$ . The total transition metal content was fixed to be unity. The residual sodium ions are believed to be present with the lithium ions in the material obtained after the ion-exchange since XRD data indicates that the starting sodium precursor phase ( $\text{Na}_{0.9}\text{Ni}_{0.45}\text{Ti}_{0.55}\text{O}_2$ ) is not present anymore after the ion-exchange. This is indicated by the slightly larger values of a and c lattice parameters than the trends obtained by Kim & Amine[12]. An accurate Rietveld refinement of site occupancies was not possible due to the relatively broad peaks in the pattern. These are likely caused by an inhomogeneous cation distribution with residual sodium in each particle after the ion-exchange. The Na content was independent of ion exchange conditions in the range of times (12-48 hours) and temperatures ( $120$ - $157^\circ\text{C}$ ) tested. However, the relative ratio of the (003) and the (104) peaks systematically decreased as the temperature and the time of the ion exchange process increased. From Figure 3((a)-(b)) and 3((c)-(d)), it can be seen that for a fixed ion exchange time, an increase in ion exchange temperature leads to a decrease in the ratio of the (003) to (104) peaks. Similarly, a decrease in exchange time leads to an observable increase in the ratio of the (003)/(104) peak intensities at a fixed temperature (e.g. compare pattern 3((a), (d)) and 3((b), (c)). It is known that the ratio value of (003)/(104) peak intensities decreases as the degree of cations mixing increases in the layered structure [3]. Therefore, our data indicate that longer time and higher temperature ion-exchange induces more cation disordering. When we tried to directly synthesize  $\text{Li}_{0.9}\text{Ni}_{0.45}\text{Ti}_{0.55}\text{O}_2$  from solid-state reaction, the totally disordered Fm3m phase formed (Figure 3(e)) in agreement

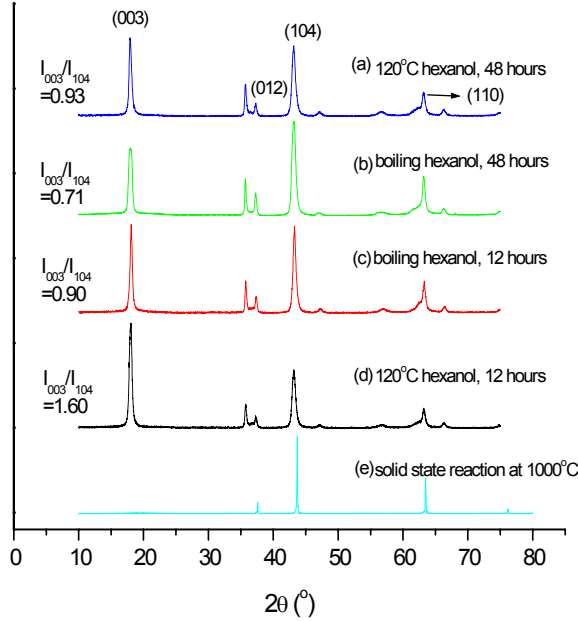


**Fig. 3** XRD of  $\text{Li}_{0.9}\text{Ni}_{0.45}\text{Ti}_{0.55}\text{O}_2$  obtained from different synthesis conditions

with the work by Chang [7]. This indicates that disordering of cations is favored at elevated temperature.

We obtained further confirmation that prolonged high temperature exposure leads to more transition metal mixing into the Li layer by taking one of the best layered samples and heating it in air to  $160^\circ\text{C}$ , which caused the 003/104 intensity ratio to decrease further (Fig.4).

From the series of synthesis trials, we believe that the 12 hours ion-exchange at  $120^\circ\text{C}$  yielded the best layered structure.

We also investigated the ideal structure with  $\text{Ni}/\text{Ti}=1$ ,  $\text{Li}(\text{Ni}_{0.5}\text{Ti}_{0.5})\text{O}_2$ , using first principles calculations in the Spin-polarized Generalized Gradient Approximation to Density Functional Theory. Further computational details are not given in this paper, as they are similar to previous work [4] on related materials. Calculations on periodic supercells require one to adopt an ordered configuration for the Ni and Ti ions. The smallest supercell has two formula units and can have Ni and Ti ordered in either rows along one of the hexagonal axis, or zig-zag configurations. We tested both, but found no significant difference between them for the results reported here (voltage, oxidation states, electronic structure). To determine the oxidation states, the electron spin is integrated around Ni and Ti. The result in Fig. 5(b) gives no unpaired electrons for Ti and about 1.5 spin for Ni, corresponding to  $\text{Ti}^{4+}$  and  $\text{Ni}^{+2}$  approximately considering the some electron loss to the oxygen  $p$  orbital. Partial delithiation (Fig. 5(a)) clearly leads to a decrease in spin density of Ni, indicating that  $\text{Ni}^{+2}$  is oxidized to  $\text{Ni}^{+3}$ . Further

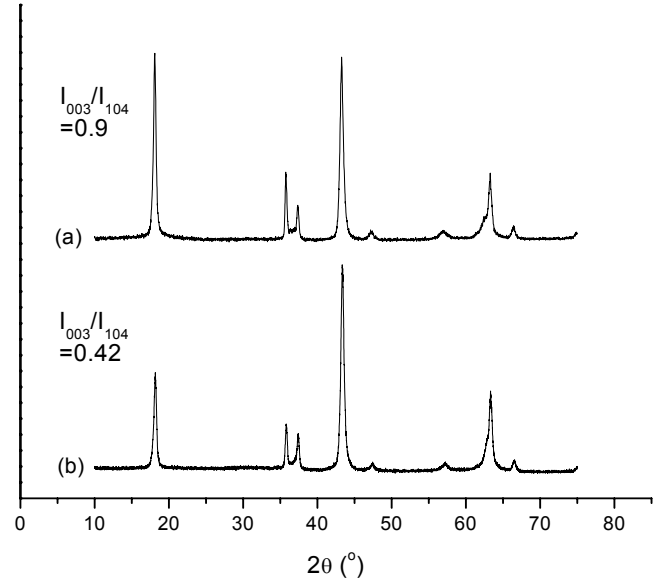


**Fig. 4** (a)  $\text{Li}_{0.9}\text{Ni}_{0.45}\text{Ti}_{0.55}\text{O}_2$  synthesized in boiling hexanol for 12 hours (b) after heating in oven at  $160^\circ\text{C}$  for 2 days.

Li removal was found to lead to  $\text{Ni}^{+4}$ . This result is similar to the  $\text{LiNi}_{0.5}\text{Mn}_{0.5}\text{O}_2$  system where the redox couple is  $\text{Ni}^{+2}/\text{Ni}^{+4}$  while Mn acts only as a structure stabilizer [4]. Based on the  $\text{Ni}^{+2}/\text{Ni}^{+4}$  redox couple, the theoretical capacity is 290.6 mAh/g. The calculated average voltage between  $\text{LiNi}_{0.5}\text{Ti}_{0.5}\text{O}_2$  and  $\text{Li}_{0.5}\text{Ni}_{0.5}\text{Ti}_{0.5}\text{O}_2$  is 3.58V and the voltage between  $\text{Li}_{0.5}\text{Ni}_{0.5}\text{Ti}_{0.5}\text{O}_2$  and  $\text{Ni}_{0.5}\text{Ti}_{0.5}\text{O}_2$  is 3.84V. Given that GGA calculations have been found to underestimate the voltage of the  $\text{Ni}^{+2}/\text{Ni}^{+4}$  redox couple by about 0.7V, the charging voltage for  $\text{LiNi}_{0.5}\text{Ti}_{0.5}\text{O}_2$  may actually be quite high. [4]

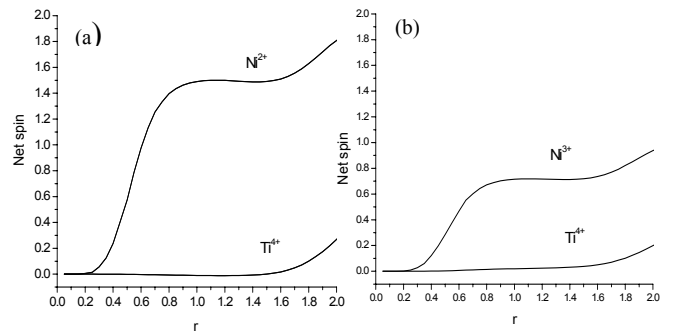


**Fig. 5** The integrated spin as a function of integration radius (Å) around Ni and Ti in (a)  $\text{LiNi}_{0.5}\text{Ti}_{0.5}\text{O}_2$  and (b)  $\text{Li}_{0.5}\text{Ni}_{0.5}\text{Ti}_{0.5}\text{O}_2$ .

The electrochemical properties of three samples with different degrees of cation disordering were evaluated (Fig. 6). The first charging capacities were about 110-150 mAh/g

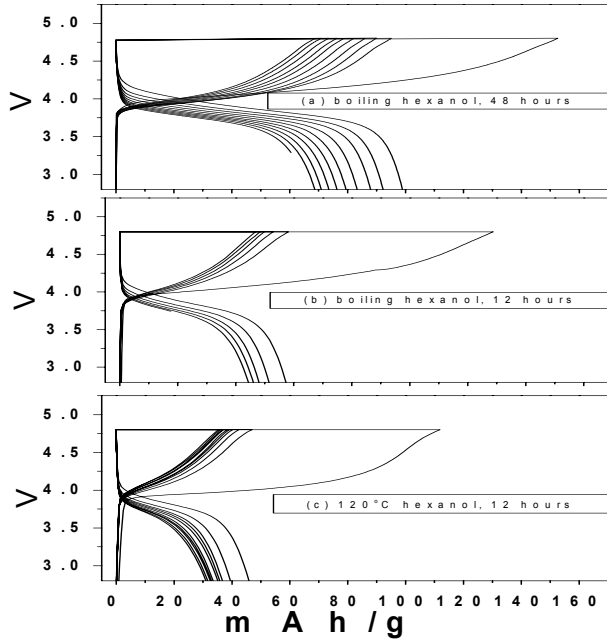


Fig. 6 galvanostatic cycling of  $\text{Li}_{0.9}\text{Ni}_{0.45}\text{Ti}_{0.55}\text{O}_2$  samples

and the first discharge capacities were about 45-95 mAh/g at C/50 rate indicating a significant capacity loss in the first cycle. Assuming that electrochemical redox couple is  $\text{Ni}^{+2}/\text{Ni}^{+4}$  in this material, the first charging capacity is far less than the theoretical capacity (265.1 mAh/g for  $\text{Li}_{0.9}\text{Ni}_{0.45}\text{Ti}_{0.55}\text{O}_2$ ).

The origin of the low capacity and significant capacity loss at the first cycle could lie in several factors. The poor capacity might be explained by the low electronic conductivity of this material. Several indirect attempts were made to evaluate the conductivity. One of them was to deduce information on conductivity from the calculated density of states of the lithiated and the partially delithiated states of this material. While band gaps are notoriously unreliable in LDA or GGA, some information on conductivity can be deduced from the nature of the occupied and lowest unoccupied states. Figure 7 shows the electronic density of states for  $\text{LiNi}_{0.5}\text{Ti}_{0.5}\text{O}_2$  and  $\text{Li}_{0.5}\text{Ni}_{0.5}\text{Ti}_{0.5}\text{O}_2$ . In  $\text{LiNi}_{0.5}\text{Ti}_{0.5}\text{O}_2$ , the Fermi-level resides in a gap between the filled majority spin Ni  $e_g$  states and the unfilled minority spin Ni  $e_g$ . In  $\text{Li}_{0.5}\text{Ni}_{0.5}\text{Ti}_{0.5}\text{O}_2$ , the Fermi-level is in the pseudo-gap between Ni  $e_g$  states. Clearly at both Li compositions, the Ti states are rather far removed from the Fermi-level, and it is, therefore, likely that only Ni participates in the electronic conductivity in this material. Given that Ni occupies less than 50% of the transition metal layer positions and is randomly distributed, Ti rich region can act to reduce electronic transport. We could not perform a direct electronic conductivity measurement on the samples as sintering them leads to irreversible structural changes.

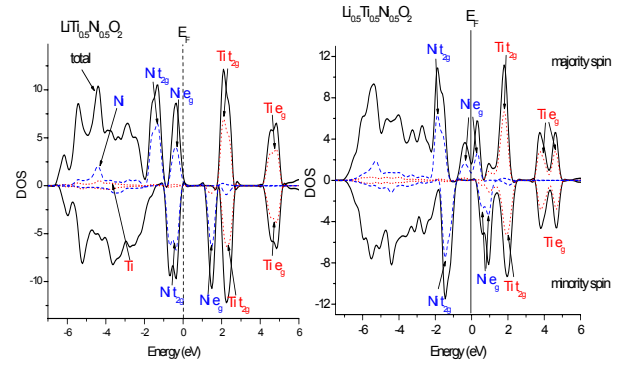
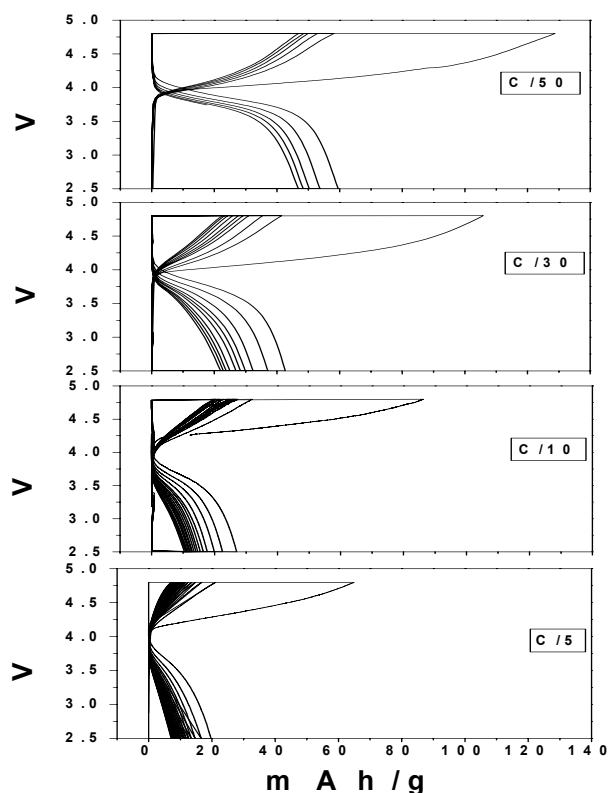


Fig. 7 The spin density of state of the 3d orbitals of Ni and Ti in  $\text{LiNi}_{0.5}\text{Ti}_{0.5}\text{O}_2$  and  $\text{Li}_{0.5}\text{Ni}_{0.5}\text{Ti}_{0.5}\text{O}_2$ .

We also compared the specific capacities at different C rates. As shown in Figure 8, the capacity reduces dramatically with increasing C-rate, consistent with some transport limitation in the material. Moreover, the large potential drop after the first charging indicates that there is a large resistance in the cell, which we attribute to the large resistance of the positive electrode.

Surprisingly, the samples that are believed to be the most layered suffer the largest first-cycle capacity loss. While in-situ or post-cycling ex-situ XRD studies are required to clarify the structural changes associated with the capacity loss, we speculate that it may be related to  $\text{Ti}^{4+}$  migration into the Li layer, as has been observed for  $\text{Na}_x\text{TiO}_2$  [14]. Since  $\text{Ti}^{4+}$  has no d-electrons, ligand-field effects do not contribute to any octahedral stabilization energy. This may make Ti migration into the Li layer, which requires passing through tetrahedral sites, easier [5]. Using first principles calculations, we attempted to determine the activation barrier for  $\text{Ti}^{4+}$  migration into the Li layer. For a transition metal ion to migrate into the Li layer, it needs to successively pass through an oxygen triangle connecting the octahedral site in the transition metal layer, a tetrahedral site and another oxygen triangle connecting it to the octahedral site in the Li layer. This migration path is complex with typically two maxima as the ion passes through the faces between the octahedral and tetrahedral, and a local minimum in the tetrahedral and octahedral sites. A Li tri-vacancy was always present in the calculations, as transition metals will not move into the tetrahedral site unless the three Li sites that share faces with it are vacant. Such tri-vacancies occur frequently at high states of charge. The result revealed a complicated dependence of  $\text{Ti}^{4+}$  stability on its local environment. Overall,  $\text{Ti}^{4+}$  migration was easiest when surrounded by other  $\text{Ti}^{4+}$ . In  $\text{Li}_{0.5}\text{TiO}_2$ , a tetrahedral Ti defect actually lowers the energy by about 0.15 eV. As Ti becomes surrounded by more  $\text{Ni}^{+2}$ , we found that migration of Ti into the tetrahedral site becomes unfavorable due to the strong



**Fig. 8 galvanostatic cycling of  $\text{Li}_{0.9}\text{Ni}_{0.45}\text{Ti}_{0.55}\text{O}_2$  sample (boiling hexanol, 12 hours) at different C rate**

electrostatic effective attraction between  $\text{Ti}^{4+}$  and  $\text{Ni}^{+2}$  in the transition metal layer. A  $\text{Ti}^{4+}$  surrounded by only  $\text{Ni}^{+2}$  requires about 0.45eV to go into the tetrahedral site. This may explain why small amounts of Ti doping in  $\text{LiNiO}_2$  result in a very stable material with little capacity fade [9].

Given the high concentration of  $\text{Ti}^{4+}$  in our sample,  $\text{Ti}^{4+}$  migration into the Li layer seems likely for the well-ordered samples (Fig.6(c) and (b)). If the sample already has immobile transition metal ions in the layer, the probability that tri-vacancies occur in the Li layer during charging is significantly reduced. As a result, less  $\text{Ti}^{4+}$  migration is expected during cycling. This may explain why the more disordered sample actually has smaller first-cycle capacity loss.

#### IV. CONCLUSIONS

We have successfully synthesized layered  $\text{Li}_{0.9}\text{Ni}_{0.45}\text{Ti}_{0.55}\text{O}_2$  through ion-exchange from  $\text{Na}_{0.9}\text{Ni}_{0.45}\text{Ti}_{0.55}\text{O}_2$ . The material has a significant tendency for transition metal cation mixing into the Li layer as evidenced by the disordered product obtained in direct high temperature synthesis of the Li compound. This disordering also limits the time and temperature of the ion-exchange process, and may be the root cause of the significant first-cycle capacity loss. Based upon the results of first

principles calculations, we believe this capacity loss to be due to  $\text{Ti}^{4+}$  migration into the Li layer, though further structural characterization is required to demonstrate this conclusively.

#### ACKNOWLEDGMENT

The authors would like to thank Prof. Clare Grey, Dr. Laurence Croguennec and Prof. Claude Delmas for the valuable discussion. This work was supported by the MRSEC Program of the National Science Foundation under award number DMR 02-13282, by the Assistant Secretary for Energy Efficiency and Renewable Energy, Office of FreedomCAR and Vehicle Technologies of the U.S. Department of Energy under Contract No. DE-AC03-76SF00098, Subcontract No. 6517748 with the Lawrence Berkeley National Laboratory and by the US-France cooperative agreement NSF-INT-0003799. The authors are grateful to Prof. Bingjo Hwang, Dr. Dane Morgan, Dr. Eric Wu and Dr. Anton Van der Ven for the priceless advice.

#### REFERENCES

- [1]. Z. Lu, D. D. MacNeil, and J. R. Dahn, *Electrochemical and Solid State Letters* **4**, A191 (2001)
- [2]. B. Ammundsen and J. Paulsen, *Adv. Mater.* **13**, 943 (2001).
- [3]. J. Reed, G. Ceder, *Electrochemical and Solid State Letters* **5**(7), A145 (2002).
- [4]. J. Reed, G. Ceder, A Van der Ven, *Electrochemical and Solid State Letters* **4**(6), A78 (2001).
- [5]. E. J. Wu, P. D. Tepesch, G. Ceder, *Philosophical Magazine B* **77**(4), 1039 (1998).
- [6]. S.H. Chang, S.G Kang, S.W. Song, J.B Yoon, J.H. Choy, *Solid State Ionics* **86-88**, 171 (1996).
- [7]. L. Croguennec, E. Suard, P. Willmann, C. Delmas, *Chem. Mater.* **14**, 2149 (2002).
- [8]. J. Kim, K. Amine, *Electrochemistry Communication* **3**, 52 (2001)
- [9]. V B Nalbandyan, I L Shukaev, *Russian Journal of Inorganic Chemistry* **37**(11), 1231 (1992).
- [10] Y.J. Shin, M.Y. Yi, *Solid State Ionics* **132**, 131 (2000).
- [11] J. Kim, K. Amine, *Journal of Power Sources* **104**, 33 (2002)

**Kisuk Kang** was born in Korea. He received his BS degree in Department of Materials Science and Engineering at Seoul National University in 2001. He started his Ph. D program in Department of Materials Science and Engineering at MIT in 2001

He is currently working as a Research Assistant in Prof. Ceder's group in MIT and doing his research mainly on cathode materials in Li ion Batteries through experiments and simulations using First Principles calculation.